Ab Initio Study of Water Adsorption and Reactivity on the (211) Surface of Anatase TiO_2

Jing Xu,[1] Li-Fang Xu,[2,*] Zhen-Zhen Li,[2] Jian-Tao Wang,[2,3,†] Zhe-Shuai Lin,[4] Kai Liu,[1] Yong-Ge Cao,[1] and Annabella Selloni[5]

[1]*Beijing Key Laboratory of Optoelectronic Functional Materials and Micro-nano Devices, Department of Physics, Renmin University of China, Beijing 100872, China*
[2]*Beijing National Laboratory for Condensed Matter Physics, Institute of Physics, Chinese Academy of Sciences, Beijing 100190, China*
[3]*School of Physics, University of Chinese Academy of Sciences, Beijing 100049, China*
[4]*Technical Institute of Physics and Chemistry, Chinese Academy of Sciences, Beijing 100190, China*
[5]*Department of Chemistry, Princeton University, Princeton, New Jersey 08544, USA*

(Received 31 March 2016; published 7 June 2016)

The reactivity of the anatase TiO_2 (211) surface is systematically studied by *ab initio* calculations of the surface energy and water-adsorption energy. We find that anatase (211) has a high surface energy of 0.97 J/m^2, close to that of the (001) surface, and the unsaturated fourfold-coordinated Ti_4 atom is more reactive than the unsaturated fivefold-coordinated Ti_5 atom. Accordingly, for water adsorption on the (211) surface, a dissociative form is favored on Ti_4 sites, with a large adsorption energy $\Delta H_{H,OH} \sim 1.28$ eV, while a nondissociative molecular form is favored on Ti_5 sites, with a smaller adsorption energy $\Delta H_{H_2O} \sim 0.78$ eV. Such distinct surface properties lead to a mixed dissociative and molecular adsorption configuration when the coverage is increased from 1/3 to 1 monolayer. These results suggest that, similar to the (001) surface, the anatase (211) surface exhibits high reactivity and may be useful in catalytic and photocatalytic applications as well.

DOI: 10.1103/PhysRevApplied.5.064001

I. INTRODUCTION

Titanium dioxide (TiO_2) has been the most intensively investigated binary transition-metal oxide in the past four decades since the discovery of photocatalytic splitting of water on a TiO_2 electrode in 1972 [1]. As a major polymorph of TiO_2, anatase TiO_2 is the most widely studied phase and is extensively used in many industrial applications such as photovoltaic cells, photo- and electrochromics, photocatalysis, photonic crystals, smart surface coatings, and sensors [1–8]. In all applications, the surface structure plays a key role, as the surface reactivity and physicochemical properties depend strongly on the exposed crystallographic facet. Therefore, the search for high-reactivity surfaces of anatase TiO_2 is a topic of great interest and an area of intense activity.

Many studies of the anatase TiO_2 surface focus on the (001) and (101) surfaces [9–17]. Theoretical studies [11–15] show that the (101) surface is the thermodynamically most stable surface with a small surface energy of 0.49 J/m^2, while the (001) surface is the highest-reactivity surface with a high surface energy of 0.98 J/m^2. Inspired by these theoretical findings, high-purity anatase TiO_2 with a large percentage of (001) facets has been synthesized using wet chemical methods with fluorine-containing species [16]. More recently, using different dopants, adsorbates, or solvated species, anatase TiO_2 nanocrystals exposing various crystalline facets have been prepared, including low-index facets such as (100) [18–21], (010) [22–24], (101) [24–30], (110) [31], and (111) [32], and high-index facets such as (103), (105), (106), (201), (301), and (401) [33–37].

The interaction of TiO_2 surfaces with water is of special interest. The structure of the hydrated surfaces is important not only because water is always present on anatase TiO_2 surfaces, but also because it can help understand and control the catalytic and (photo-) electrochemical properties of this material. In fact, different water-adsorption states have been found; e.g., water favors molecular adsorption on the anatase (101) surface and dissociative adsorption on the (001) surface [14]. Very recently, a large percentage of exposed (211) facet has been identified by x-ray diffraction on N-doped TiO_2 films prepared by rf reactive magnetron sputtering [38]. It is found that the increase of exposed (211) facets can effectively improve the photocatalytic activity of TiO_2 for water-dissociation reactions [39]. However, the origin of the reactivity of the anatase (211) surface remains largely to be explored.

*Corresponding author.
lfxu@iphy.ac.cn
†Corresponding author.
wjt@aphy.iphy.ac.cn

Motivated by these recent experimental findings, in this work we present a systematic study of the surface reactivity and water adsorption on anatase (211) using *ab initio* calculations. We find that anatase (211) has a high surface energy of 0.97 J/m^2, close to our computed value of 1.08 J/m^2 for the (001) surface. A distinctive feature of anatase (211) is the presence of both Ti_4 atoms, with two unsaturated bonds, and Ti_5 atoms, with one unsaturated bond. Our results show that water adsorbs dissociatively on Ti_4 sites, while nondissociative molecular water adsorption takes place on Ti_5 sites. The detailed structures and stabilities of adsorbed water on the anatase TiO_2 (211) surface are discussed for increasing water coverage from 1/3 to 1 monolayer (ML).

II. METHOD AND MODELS

Calculations are performed by the Vienna *ab initio* simulation package (VASP) [40–42] with the all-electron projector-augmented-wave method [43]. The generalized-gradient approximation [44] is set as the exchange and correlation functional. The valence states $3d^24s^2$ for Ti, $2s^22p^4$ for O, and $1s^1$ for H are used with an energy cutoff of 500 eV for the plane-wave basis set. The calculated lattice constants for bulk anatase TiO_2 are used to construct the diverse facets listed in Table I. The anatase (211) surface is modeled by a slab of six layers with a unit surface cell of 7.706 Å × 5.501 Å × 27.677 Å ($\gamma = 101.44°$) comprising a total of 54 atoms separated by a vacuum region of 12 Å. The Monkhorst-Pack scheme [45] is adopted for the Brillouin-zone integration with a $6 \times 6 \times 1$ k-point mesh. All the atoms are relaxed during geometry optimizations with the given surface cell. Convergence criteria employed for both the electronic self-consistent relaxation and the ionic relaxation are set to 10^{-6} eV and 0.01 eV/Å for the total energy and Hellmann-Feynman force, respectively.

III. RESULTS AND DISCUSSION

A. Surface structures and energetics

We first study the surface structure and energetics. The stoichiometric unrelaxed termination of the (211) surface is shown in Fig. 1(a). There are five undercoordinated and four fully coordinated atoms exposed to the vacuum. The five undercoordinated atoms include three inequivalent twofold-coordinated oxygen atoms denoted by O_{21}, O_{22}, and O_{23}, a fourfold-coordinated Ti_4, and a fivefold-coordinated Ti_5, respectively. The four fully coordinated atoms are O_{31}, O_{32}, O_{33}, and Ti_6 [see Fig. 1(a)]. Different from (001) and (101) surfaces [14], fourfold-coordinated Ti_4 atoms are thus present on the (211) surface. The two undercoordinated Ti atoms connect via the O_{22} atom forming an angle $\angle Ti_4{-}O_{22}{-}Ti_5 = 101.9°$, while Ti_5 and bulk Ti_6 atoms are connected via the O_{31} atom forming an angle $\angle Ti_5{-}O_{31}{-}Ti_6 = 156.2°$ as in bulk anatase [15]. Meanwhile, there are four different bond angles, notably $\angle O{-}Ti{-}O = 78.10°$, 92.44°, 101.90°, and 156.20° in bulk anatase.

Figure 1(b) shows the optimized anatase (211) surface. After relaxation, the (211) surface shows a very corrugated structure, with a characteristic sawtoothlike profile along the [1-31] direction. All undercoordinated oxygen (O_{2i}) atoms are displaced outward, while the undercoordinated Ti_4 and Ti_5 atoms are relaxed inward. Both angles $\angle Ti_4{-}O_{22}{-}Ti_5$ and $\angle Ti_5{-}O_{31}{-}Ti_6$ become smaller: 100.3° and 147.7°, respectively. The largest relaxations are those of the fully coordinated oxygen O_{31}, which relaxes outward by approximately 0.35 Å, and O_{32}, which relaxes inward by approximately 0.34 Å. Note that here the surface atoms form four-membered-ring (O—Ti—O—Ti) structures on the surface. These O—Ti—O—Ti rings are slightly deformed, and the distances between oxygen atoms in the rings increase from the bulk value of 2.458 to 2.492–2.515 Å.

TABLE I. Calculated surface energies (E in J/m^2) and surface densities of fivefold-coordinated Ti_5, fourfold-coordinated Ti_4, and twofold-coordinated oxygen O_2 atoms [$n(Ti_5)$, $n(Ti_4)$, and $n(O_2)$]. N_{at} is the total number of atoms in the slab.

Facet	N_{at}	E (J/m^2)	$n(Ti_5)$	$n(Ti_4)$ (10^{-2} Å^{-2})	$n(O_2)$
(101)	24	0.52	5.1		5.1
(001)	18	1.08	6.9		6.9
(211)	54	0.97	2.4	2.4	7.2
$(103)_s$ [15]	48	0.99		3.5	
(110) [15]	42	1.15		3.8	

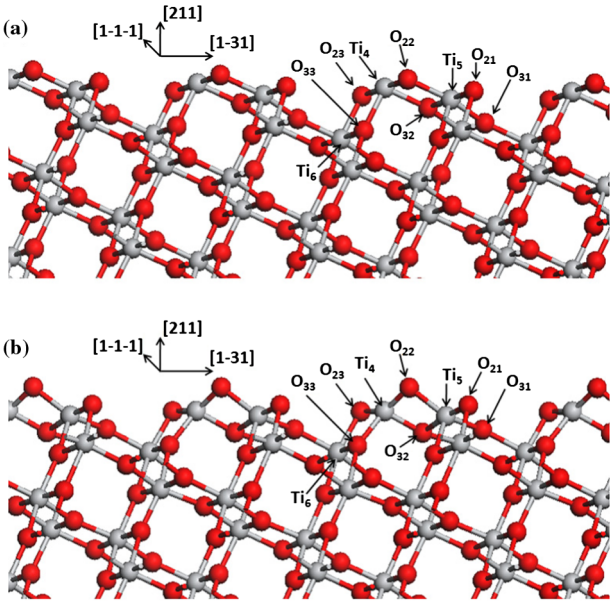

FIG. 1. Structures of the unrelaxed (a) and relaxed (b) anatase (211) surfaces. The O and Ti atoms are in red and gray spheres, respectively, indicated with different coordination numbers.

To understand the surface stability, the surface energies for (101), (001), and (211) are estimated using the following expression:

$$E = \frac{(E_{\text{tot}} - nE_{\text{bulk}})}{A}, \tag{1}$$

where E_{tot} is the total energy of the slab and E_{bulk} is the energy of TiO_2 unit in the bulk, n is the number of TiO_2 units in the slab, and A is the total surface area of the slab, including both sides of the slab. The calculated surface energies are listed in Table I. The surface energy of the (001) surface is estimated to be 1.08 J/m^2, which is nearly twice that of the most stable anatase (101) surface (0.52 J/m^2), in agreement with previous theoretical studies [15]. Similarly, the (211) surface has a high surface energy of 0.97 J/m^2, close to that of the (001) surface.

The value of the surface energy is known to be strongly correlated to the presence of undercoordinated Ti atoms on the surface [15]. The (001) surface energy is large because of the high surface density of Ti_5 (see Table I). However, the surface energy of anatase (211) is large even though the total density of undercoordinated Ti_4 and Ti_5 atoms is smaller than that on the (001) surface [even smaller than on (101)]. This result suggests that Ti_4 atoms, with two unsaturated bonds, have a higher reactivity than Ti_5 atoms with one unsaturated bond. A similar behavior is also found for the anatase (110) and $(103)_s$ surfaces [15].

B. Water adsorption

We next investigate the adsorption of water on the TiO_2 (211) surface at various coverages $\theta = 1/3, 2/3$, and 1 ML, by considering one, two, and three adsorbed water molecules per surface unit cell, respectively. For a single water molecule (1/3 ML), there are four possible adsorption modes, corresponding to different adsorption positions (Ti_4 or Ti_5) and different (molecular or dissociative) adsorption conformations. For *molecular water adsorption on a* Ti_5 *site* [see Fig. 2(a)], the oxygen of water bonds to Ti_5 with a bond length of 2.226 Å, and two surface oxygen atoms via Ti_5 form two bond angles $\angle O_{\text{water}}{-}Ti_5{-}O_{22} = 99.85°$ and $\angle O_{\text{water}}{-}Ti_5{-}O_{31} = 77.18°$, close to the bulk angles of 101.90° and 78.10°, respectively. Upon water adsorption, the Ti_5 site becomes sixfold coordinated: The Ti atom has six Ti–O bonds with their orientations similar to those in the bulk. At the same time, the two hydrogen atoms of water form H bonds (HBs) with two neighboring surface undercoordinated oxygen atoms, O_{21} and O_{23}, with bond lengths 2.339 and 1.873 Å, respectively. As a result, the computed molecular-adsorption energy on the Ti_5 site is 0.784 eV. For *dissociative water adsorption on a* Ti_5 *site* [see Fig. 2(b)], the water molecule is dissociated into hydroxyl (OH) and H fragments. The two bond angles are $\angle O_{\text{OH}}{-}Ti_5{-}O_{22} = 99.70°$ and $\angle O_{\text{OH}}{-}Ti_5{-}O_{31} = 86.73°$, respectively. The OH group bonds to Ti_5 with a length of 1.857 Å and then further bonds to O_{23} with a weak HB (length 2.394 Å). The H fragment forms a new OH moiety with a nearby O_{21} (OH length 0.999 Å). As a result, the adsorption energy for a dissociated water on a Ti_5 site is 0.77 eV, which is slightly smaller than that of molecular adsorption. Thus, molecular adsorption is slightly preferred on a Ti_5 site. On the other hand, for *molecular water on a* Ti_4 *site* [see Fig. 2(c)], the oxygen atom of water binds to Ti_4 with a bond length of 2.207 Å, and one hydrogen atom forms a HB with a neighboring O_{21} atom, with a length of

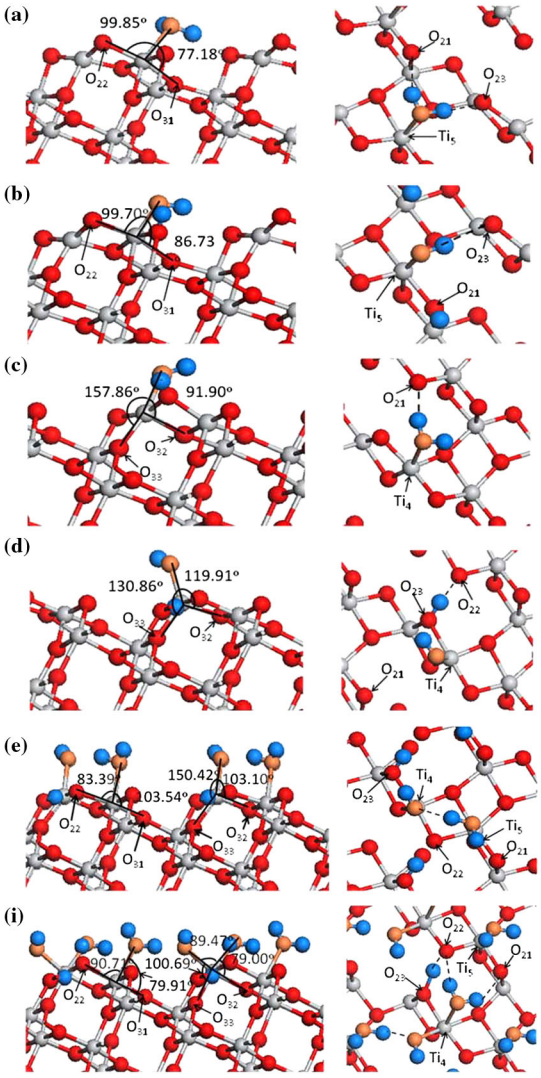

FIG. 2. Side (left) and top (right) views of the structures for water adsorption on the anatase TiO_2(211) surface. (a) Molecular water on a Ti_5 site. (b) Dissociative water on a Ti_5 site. (c) Molecular water on a Ti_4 site. (d) Dissociative water on a Ti_4 site. (e) Mixed state with one dissociative H_2O on Ti_4 and one molecular H_2O on Ti_5 sites at 2/3 ML. (i) Mixed water adsorption with one dissociative water on Ti_4, one molecular water on Ti_4, and one molecular water on Ti_5 sites at 1-ML coverage. The O atom of water is plotted in orange, the H atom is in blue, and the H bond is indicated by a dashed line.

1.869 Å. Note the bond angles $\angle O_{water}—Ti_4—O_{33} = 157.86°$ and $\angle O_{water}—Ti_4—O_{32} = 91.90°$, close to the bulk angles of 156.20° and 92.44°, respectively, indicating that Ti_4 is located at the position of one of the bulk Ti—O bonds. The Ti_4 adsorption site becomes fivefold coordinated, and the adsorption energy for molecular water on a Ti_4 site is estimated to be 0.99 eV. Moreover, for *dissociative water on a* Ti_4 *site* [see Fig. 2(d)], the O atom of the OH group is strongly bonded to the Ti_4 atom with a bond length of 1.847 Å (to be compared to the Ti—O bond length of 2.207 Å in the molecular-adsorption case) so that the Ti_4 adsorption site becomes fivefold coordinated. It is worthwhile to point out that the adsorption position of the O atom of the OH group does not correspond to the position of a bulk Ti—O bond but is rather in the middle of the two missing bulk Ti—O bonds, and the orientation of the $Ti_4—O_{OH}$ bond clearly *deviates from its direction in the bulk*, as shown by two bond angles $\angle O_{OH}—Ti_4—O_{33} = 130.86°$ and $\angle O_{OH}—Ti_4—O_{32} = 119.91°$. This adsorption geometry with a short bond length and a middle position indicates that the dissociated water interacts with two unsaturated Ti_4 bonds indeed. Furthermore, the hydrogen atom of OH forms a weak HB with a neighboring O_{23} atom of length 2.534 Å. The dissociated H from water interacts with a surface oxygen O_{23} forming a new OH moiety with a bond length of 1.013 Å and further forms a HB of 1.598 Å with O_{22}. As a result, the adsorption energy for dissociated water on a Ti_4 site is estimated to be 1.28 eV [46], which is significantly larger than the value of 0.99 eV obtained for molecular adsorption. Thus, dissociative adsorption is preferred at the Ti_4 site [47].

According to the above results, the adsorption energies of water on a Ti_4 site are always larger than those on a Ti_5 site (see Table II). Moreover, a water molecule can be *easily* dissociated on a Ti_4 site, while it *hardly* dissociates on Ti_5. These differences can be understood in terms of a simple model based on the bond charge distribution. In bulk anatase TiO_2, each Ti atom has six nearest-neighboring O atoms; thus, each Ti—O bond has 4/6 electron charge on average. When a Ti_4 atom interacts with the oxygen atom of H_2O, it can offer about 4/3 electron charge to this O atom by forming a strong bond [see Fig. 2(d)]. Thus, one H atom can be released from the water molecule on a Ti_4 site. In fact, one H atom dissociates spontaneously from the water molecule as it adsorbs on a Ti_4 atom. On the other hand, Ti_5 can provide only about 2/3 electron charge to the water O atom, which is less than the charge contribution from a H atom. Therefore, Ti_5 hardly causes dissociation of a H atom, and water favors molecular adsorption on a Ti_5 site. The very little difference in energy (0.014 eV) between molecular and dissociated structures is a clear indication of a strong competition between the two types of adsorption. These results confirm that four-coordinated Ti_4 atoms with two unsaturated bonds have a stronger chemical reactivity than Ti_5 atoms with one unsaturated bond. The dissociative water adsorption on a Ti_4 site is similar to that found on the (001) surface [14], where a Ti_5 atom actually becomes fourfold coordinated after breaking its bond to a bridging O_2 atom. Dissociative adsorption is also favored at step edges exposing Ti_4 atoms on anatase (101) [10].

For two adsorbed H_2O molecules (2/3 ML coverage), the first H_2O prefers to adsorb at a Ti_4 site in dissociative form according to the single water-adsorption results; next, another water molecule should adsorb on a Ti_4 or Ti_5 site. For the structure (e) with one dissociated H_2O on a Ti_4 site and one molecular H_2O on a Ti_5 site [see Fig. 2(e)], the $O—Ti_5$ bond is 2.230 Å, while the $O—Ti_4$ bond length is much shorter, 1.992 Å. The dissociated H combines with an O_{23} atom forming a new OH moiety and further forms a strong HB (1.590 Å) with an O_{22} atom. An additional HB between two water molecules forms with a bond length of 1.775 Å, which makes two water molecules closer and changes the values of the bond angles. In this mixed structure (e), the adsorption energy is 1.045 eV/mol, which is a little larger than the averaged value of 1.034 eV $[(1.284 + 0.784)/2]$ for the single water adsorption on Ti_4 and Ti_5 sites due to the contribution of the new HB. On the contrary, for the structure (f) with two dissociated H_2O on Ti_4 and Ti_5 sites, the adsorption energy is estimated to be 0.991 eV/mol, which is about 0.036 eV smaller than the averaged value of 1.027 eV $[(1.284 + 0.770)/2]$ for the single water adsorption and also 0.054 eV lower than that of the mixed configuration (e). These results confirm that *molecular adsorption is preferred on* Ti_5 in the mixed structure. Moreover, for structure (g) with one dissociated H_2O and one undissociated H_2O on Ti_4 sites and structure (h) with two dissociated H_2O on Ti_4 sites, the adsorption energy is estimated to be 0.960 and 0.916 eV/mol, respectively, which is clearly lower than 1.045 eV/mol for the mixed structure (e). Therefore, with increasing coverage, water molecules prefer to be adsorbed in a mixed form with

TABLE II. Adsorption energy (ΔH in eV) per H_2O molecule on anatase (211) at various water coverages $\theta = 1/3$, 2/3, and 1 ML. The adsorption states are shown as H_2O = molecular and H, OH = dissociative on a Ti_4 or Ti_5 site. The relative structures (a)–(l) are given Figs. 2, S1, and S2.

θ (ML)	Structure	H_2O	H,OH	ΔH (eV)
1/3	a	Ti_5		0.784
	b		Ti_5	0.770
	c	Ti_4		0.994
	d		Ti_4	1.284
2/3	e	Ti_5	Ti_4	1.045
	f		Ti_4, Ti_5	0.991
	g	Ti_4	Ti_4	0.960
	h		Ti_4, Ti_4	0.916
3/3	i	Ti_4, Ti_5	Ti_4	0.946
	j	Ti_5	Ti_4, Ti_4	0.909
	k	Ti_4	Ti_4, Ti_5	0.902
	l		Ti_4, Ti_4, Ti_5	0.883

one dissociated H_2O on a Ti_4 site and one intact H_2O on a Ti_5 site. The detailed structures (e)–(h) with two water molecules are shown in Fig. S1 in Supplemental Material [48].

Finally, we discuss the monolayer coverage where three water molecules are adsorbed per surface unit cell. Following the 2/3 ML result with one dissociated H_2O on a Ti_4 site and one molecular H_2O on a Ti_5 site, the third molecule would adsorb molecularly on a Ti_4 site [structure (i) in Fig. 2]. Its O atom binds to Ti_4 with a bond length of 2.259 Å, while the two H atoms form HBs with nearby O atoms, where $H{-}O_{21}$ is 2.156 Å and $H{-}O_{22}$ is 1.907 Å. The bond length for molecular water on a Ti_5 atom is 2.221 Å, while for dissociated water on Ti_4 it is 1.934 Å. Two bond angles $\angle O_{OH}{-}Ti_4{-}O_{33}$ and $\angle O_{water}{-}Ti_4{-}O_{32}$ are 100.69° and 79.00°, respectively. Thus, all Ti atoms are sixfold coordinated with orientations similar to those of a bulk Ti atom. The dissociated H is captured by an O_{23} atom to form an OH moiety and further interacts with an O_{22} atom forming a HB of 1.835 Å. An additional HB of 1.652 Å also exists between these two adsorbed H_2O. All surface atoms become saturated. The adsorption energy has a larger value of 0.946 eV/mol for this mixed configuration on Ti_4 sites. For comparison, we consider also configuration (j) with two dissociated water molecules on Ti_4 sites and one molecular H_2O on Ti_5. Though all surface atoms are also saturated, its adsorption energy is 0.909 eV/mol, which is lower than that of the mixed configuration with one dissociative and one molecular adsorption on Ti_4. Thus, molecular adsorption is favored on Ti_4 for the second water molecule. Meanwhile, for structure (k) with one intact water on Ti_4 and two dissociated water molecules on Ti_4 and Ti_5 sites, the computed adsorption energy is 0.902 eV/mol; for structure (l), with three dissociated water molecules on Ti_4, Ti_4, and Ti_5 sites, the adsorption energy is 0.833 eV/mol (see Table II). These results suggest that a mixed water configuration is formed at monolayer coverage, with one dissociated water on Ti_4, one molecular water on Ti_4, and one molecular water on Ti_5. The detailed structures (i)–(l) with three water molecules are shown in Fig. S2 in Supplemental Material [48].

To obtain further insight, we also compare the densities of states and projected densities of states of the bare surface and the surface with a dissociated water molecule on a Ti_4 site. We find that the electronic structure of the surface with a dissociated water molecule on a Ti_4 site is similar to that of the bare surface near the valence-band maximum (VBM) and conduction-band minimum (CBM), and, in both cases, the VBM and CBM are mainly contributed by the O-2*p* and Ti-3*d* orbital in a TiO_2 slab, respectively, resulting in a semiconductor with a band gap of approximately 2.1 eV. Moreover, the O-2*p* orbitals in the OH group are extended to a wide range between −3.2 and −0.9 eV, indicating that the O atom of OH is strongly interacting with the substrate (see Fig. S3 in Supplemental Material [48]). On the other hand, for the case with a molecular water adsorption on a Ti_4 site, all peaks from the water molecule are sharp and are simply superimposed on those of the bare surface, indicating that they interact weakly with the surface (see Fig. S4 in Supplemental Material [48]).

Many research groups focus on finding ways to produce H_2 from water and/or on the photocatalytic degradation of organic pollutants [49–52]. Experimental results reveal that H_2 is hardly detected when using pure TiO_2 films as a photocatalyst, whereas large amounts of hydrogen are produced and the amount of H_2 increases almost linearly with the irradiation time when using N-doped TiO_2 films with an increasing fraction of exposed (211) facets [39]. Moreover, it is reported that anatase TiO_2 films with (211) preferred orientation have a high photocatalytic activity for the degradation of organic dyes [50]. On the basis of this experimental information, it seems safe to conclude that a large percentage of exposed (211) facets can effectively enhance the activity of TiO_2-based photocatalysts.

It is worth noting that, besides the above results and discussions on the monolayer and submonolayer water adsorption on an anatase (211) surface, a more detailed molecular-dynamics simulation on multilayer water adsorption should be considered in the future to solve a realistic system in experiments.

IV. CONCLUSION

In conclusion, we perform a detailed *ab initio* study on the recently reported anatase (211) surface. This surface exposes both Ti_4 and Ti_5 undercoordinated atoms, which enables us to investigate their distinct reactivities. Our results show that the (211) surface is indeed a high-reactivity surface with a high surface energy of 0.97 J/m^2 similar to that of the (001) surface. In addition, the four-coordinated Ti_4 atoms with two unsaturated bonds have a stronger chemical reactivity in comparison to the Ti_5 atoms with one unsaturated bond. Studies of water adsorption suggest two distinct states of adsorbed water on the (211) surface, one related to undissociated molecular water on Ti_5 sites and the other to dissociated water on Ti_4 sites. These results indicate that the Ti_4 atoms will play a critical role in water decomposition. These properties make the (211) termination a promising surface for applications in catalysis and photocatalysis.

ACKNOWLEDGMENTS

This study was supported by the National Natural Science Foundation of China (Grants No. 11374341 and No. 11274356), the Strategic Priority Research Program of the Chinese Academy of Sciences (Grant No. XDB07000000), the Fundamental Research Funds for the Central Universities, and the Research Funds of Renmin University of China.

[1] A. Fujishima and K. Honda, Electrochemical photolysis of water at a semiconductor electrode, Nature (London) **238**, 37 (1972).

[2] B. O. Regan and M. Grätzel, A low-cost, high-efficiency solar-cell based on dye-sensitized colloidal TiO_2 films, Nature (London) **353**, 737 (1991).

[3] M. Grätzel, Photoelectrochemical cells, Nature (London) **414**, 338 (2001).

[4] A. Fujishima, X. Zhang, and D. A. Tryk, TiO_2 photocatalysis and related surface phenomena—Review, Surf. Sci. Rep. **63**, 515 (2008).

[5] Y. Li and G. A. Somorjai, Nanoscale advances in catalysis and energy applications, Nano Lett. **10**, 2289 (2010).

[6] G. Liu, H. G. Yang, J. Pan, Y. Q. Yang, G. Q. Lu, and H. M. Cheng, Titanium dioxide crystals with tailored facets, Chem. Rev. **114**, 9559 (2014).

[7] W. Q. Fang, X. Q. Gong, and H. G. Yang, On the unusual properties of anatase TiO_2 exposed by highly reactive facets, J. Phys. Chem. Lett. **2**, 725 (2011).

[8] A. Hagfeldt, G. Boschloo, L. Sun, L. Kloo, and H. Pettersson, Dye-sensitized solar cells, Chem. Rev. **110**, 6595 (2010).

[9] A. Selloni, Crystal growth—Anatase shows its reactive side, Nat. Mater. **7**, 613 (2008).

[10] X. Q. Gong, A. Selloni, M. Batzill, and U. Diebold, Steps on anatase TiO_2 (101), Nat. Mater. **5**, 665 (2006).

[11] X. Q. Gong and A. Selloni, Reactivity of anatase TiO_2 nanoparticles: The role of the minority (001) surface, J. Phys. Chem. B **109**, 19560 (2005).

[12] X. Q. Gong, A. Selloni, and A. Vittadini, Density functional theory study of formic acid adsorption on anatase TiO_2 (001): Geometries, energetics, and effects of coverage, hydration, and reconstruction, J. Phys. Chem. B **110**, 2804 (2006).

[13] U. Diebold, The surface science of titanium dioxide, Surf. Sci. Rep. **48**, 53 (2003).

[14] A. Vittadini, A. Selloni, F. P. Rotzinger, and M. Grätzel, Structure and Energetics of Water Adsorbed at TiO_2 Anatase (101) and (001) Surfaces, Phys. Rev. Lett. **81**, 2954 (1998).

[15] M. Lazzeri, A. Vittadini, and A. Selloni, Structure and energetics of stoichiometric TiO_2 anatase surfaces, Phys. Rev. B **63**, 155409 (2001).

[16] H. G. Yang, C. H. Sun, S. Z. Qiao, J. Zou, G. Liu, S. C. Smith, H. M. Cheng, and G. Q. Lu, Anatase TiO_2 single crystals with a large percentage of reactive facets, Nature (London) **453**, 638 (2008).

[17] F. D. Angelis, C. D. Valentin, S. Fantacci, A. Vittadini, and A. Selloni, Theoretical studies on anatase and less common TiO_2 phases: Bulk, surfaces, and nanomaterials, Chem. Rev. **114**, 9708 (2014).

[18] J. M. Li, K. Cao, Q. Li, and D. S. Xu, Tetragonal faceted-nanorods of anatase TiO_2 with a large percentage of active {100} facets and their hierarchical structure, CrystEngComm **14**, 83 (2012).

[19] L. Wu, B. X. Yang, X. H. Yang, Z. G. Chen, Z. Li, H. J. Zhao, X. Q. Gong, and H. G. Yang, On the synergistic effect of hydrohalic acids in the shape-controlled synthesis of anatase TiO_2 single crystals, CrystEngComm **15**, 3252 (2013).

[20] Z. C. Lai, F. Peng, Y. Wang, H. J. Wang, H. Yu, P. Liu, and H. I. Zhao, Low temperature solvothermal synthesis of anatase TiO_2 single crystals with wholly {100} and {001} faceted surfaces, J. Mater. Chem. **22**, 23906 (2012).

[21] J. M. Li and D. S. Xu, Tetragonal faceted-nanorods of anatase TiO_2 single crystals with a large percentage of active {100} facets, Chem. Commun. (Cambridge) **46**, 2301 (2010).

[22] X. K. Ding, H. C. Ruan, C. Zheng, J. Yang, and M. D. Wei, Synthesis of TiO_2 nanoparticles with tunable dominant exposed facets (010), (001) and (106), CrystEngComm **15**, 3040 (2013).

[23] B. H. Wu, C. Y. Guo, N. F. Zheng, Z. X. Xie, and G. D. Stucky, Nonaqueous production of nanostructured anatase with high-energy facets {001} or {010} facets, J. Am. Chem. Soc. **130**, 17563 (2008).

[24] J. Pan, G. Liu, G. Q. Lu, and H. M. Cheng, On the true photoreactivity order of {001}, {010}, and {101} facets of anatase TiO_2 crystals, Angew. Chem., Int. Ed. **50**, 2133 (2011).

[25] D. Wu, Z. Gao, F. Xu, J. Chang, S. Gao, and K. Jiang, Anatase TiO_2 nanocrystals enclosed by well-defined crystal facets and their application in dye-sensitized solar cell, CrystEngComm **15**, 516 (2013).

[26] T. R. Gordon, M. Cargnello, T. Paik, F. Mangolini, R. T. Weber, P. Fornasiero, and C. B. Murray, Nonaqueous synthesis of TiO_2 nanocrystals using TiF_4 to engineer morphology, oxygen vacancy concentration, and photocatalytic activity, J. Am. Chem. Soc. **134**, 6751 (2012).

[27] N. Wu, J. Wang, D. N. Tafen, H. Wang, J.-G. Zheng, J. P. Lewis, X. Liu, S. S. Leonard, and A. Manivannan, Shape-enhanced photocatalytic activity of single-crystalline anatase TiO_2 (101) nanobelts, J. Am. Chem. Soc. **132**, 6679 (2010).

[28] C. Chen, R. Hu, K. Mai, Z. Ren, H. Wang, G. Qian, and Z. Wang, Shape evolution of highly crystalline anatase TiO_2 nanobipyramids {001} and {101} facets, Cryst. Growth Des. **11**, 5221 (2011).

[29] J. H. Pan, G. Han, R. Zhou, and X. S. Zhao, Hierarchical N-doped TiO_2 hollow microspheres consisting of nanothorns with exposed anatase {101} facets, Chem. Commun. (Cambridge) **47**, 6942 (2011).

[30] B. Horvat, A. Rečnik, and G. Dražić, The growth of anatase bipyramidal crystals during hydrothermal synthesis, J. Cryst. Growth **347**, 19 (2012).

[31] M. Liu, L. Piao, L. Zhao, S. Ju, Z. Yan, T. He, C. Zhou, and W. J. Wang, Anatase TiO_2 single crystals with exposed {001} and {110} facets: Facile synthesis and enhanced photocatalysis, Chem. Commun. (Cambridge) **46**, 1664 (2010).

[32] H. Xu, P. Reunchan, S. X. Ouyang, H. Tong, N. Umezawa, T. Kako, and J. H. Ye, Anatase TiO_2 single crystals exposed with high-reactive {111} facets toward efficient H_2 evolution, Chem. Mater. **25**, 405 (2013).

[33] W. G. Yang, Y. Y. Xu, Y. Tang, C. Wang, Y. J. Hu, L. Huang, J. Liu, J. Luo, H. B. Guo, Y. G. Chen, W. M. Shi, and Y. L. Wang, Three-dimensional self-branching anatase TiO_2 nanorods: Morphology control, growth mechanism and dye-sensitized solar cell application, J. Mater. Chem. A **2**, 16030 (2014).

[34] H. B. Jiang, Q. Cuan, C. Z. Wen, J. Xing, D. Wu, X.-Q. Gong, C. Li, and H. G. Yang, Anatase TiO_2 crystals with exposed high-index facets (105), Angew. Chem., Int. Ed. **50**, 3764 (2011).

[35] L. Wu, H. B. Jiang, F. Tian, Z. Chen, C. Sun, and H. G. Yang, $Ti_{0.89}Si_{0.11}O_2$ single crystals bound by high-index {201} facets showing enhanced visible-light photocatalytic hydrogen evolution, Chem. Commun. (Cambridge) **49**, 2016 (2013).

[36] M. H. Yang, P. C. Chen, M. C. Tsai, T. T. Chen, I. C. Chang, H. T. Chiu, and C. Y. Lee, Alkali metal ion assisted synthesis of faceted anatase TiO_2 {101} and {301} exposed were synthesized, CrystEngComm **15**, 2966 (2013).

[37] H. B. Wu, J. S. Chen, X. W. Lou, and H. H. Hng, Asymmetric anatase TiO_2 nanocrystals with exposed high-index facets and their excellent lithium storage properties, Nanoscale **3**, 4082 (2011).

[38] C. Wang, Q. Q. Hu, J. Q. Huang, L. Wu, Z. H. Deng, Z. G. Liu, Y. Liu, and Y. G. Cao, Efficient hydrogen production by photocatalytic water splitting using N-doped TiO_2 film, Appl. Surf. Sci. **283**, 188 (2013).

[39] C. Wang, Q. Q. Hu, J. Q. Huang, Z. H. Deng, H. L. Shi, L. Wu, Z. G. Liu, and Y. G. Cao, Effective water splitting using N-doped TiO_2 films: Role of preferred orientation on hydrogen production, Int. J. Hydrogen Energy **39**, 1967 (2014).

[40] G. Kresse and J. Hafner, *Ab initio* molecular dynamics for liquid metals, Phys. Rev. B **47**, 558 (1993).

[41] G. Kresse and J. Furthmüller, Efficiency of ab-initio total energy calculations for metals and semiconductors using a plane-wave basis set, Comput. Mater. Sci. **6**, 15 (1996).

[42] G. Kresse and J. Furthmüller, Efficient iterative schemes for *ab initio* total-energy calculations using a plane-wave basis set, Phys. Rev. B **54**, 11169 (1996).

[43] P. E. Blöchl, Projector augmented-wave method, Phys. Rev. B **50**, 17953 (1994).

[44] Y. Wang and J. P. Perdew, Correlation hole of the spin-polarized electron gas, with exact small-wave-vector and high-density scaling, Phys. Rev. B **44**, 13298 (1991).

[45] H. J. Monkhorst and J. D. Pack, Special points for Brillouin-zone integrations, Phys. Rev. B **13**, 5188 (1976).

[46] There are three adsorption sites of dropped H on the surface oxygen atoms for dissociative water on a Ti_4 site. The calculated adsorption energy is 1.28 eV on O_{23}, 1.23 eV on O_{22}, and 0.92 eV on O_{21}, respectively. It is shown that the structure (d) is energetically more favorable.

[47] We check all the results listed in Table II by performing additional calculations that include the van der Waals corrections. For example, the calculated adsorption energy for a dissociated water on Ti_5 site is 0.920 eV, which is slightly smaller than the energy, 0.932 eV, of molecular adsorption; the calculated adsorption energy for a dissociated water on Ti_4 site is 1.493 eV, which is clearly larger than 1.017 eV of molecular adsorption. Thus, the van der Waals corrections do not affect our conclusion in this work.

[48] See Supplemental Material at http://link.aps.org/supplemental/10.1103/PhysRevApplied.5.064001 for the two (Fig. S1) and three (Fig. S2) water-molecule-adsorption structures on anatase TiO_2 (211) surface; also, a comparison between the density of states (and projected density of states) of the bare surface and of the one with the dissociated water molecule on a Ti_4 site (Fig. S3) and a comparison between the bare surface and the structure with a molecular water adsorption on a Ti_4 site (Fig. S4) are given.

[49] K. Ali, S. A Khan, and M. Z. M. Jafri, Structural and optical properties of ITO/TiO_2 anti-reflective films for solar cell applications, Nanoscale Res. Lett. **9**, 175 (2014).

[50] J. Y. Zheng, S. H. Bao, Y. Guo, and P. Jin, TiO_2 films prepared by DC reactive magnetron sputtering at room temperature: Phase control and photocatalytic properties, Surf. Coat. Technol. **240**, 293 (2014).

[51] L. Romero, C. Piccirillo, P. M. L. Castro, C. Bowman, M. E. A. Warwick, and R. Binions, Titanium dioxide thin films deposited by electric field-assisted CVD: Effect on antimicrobial and photocatalytic properties from (101) to (004) or (211) planes, Chem. Vap. Deposition **21**, 63 (2015).

[52] M. Zhao, H. Xu, H. R. Chen, S. X. Ouyang, N. Umezawa, D. F. Wang, and J. H. Ye, Photocatalytic reactivity of {121} and {211} facets of brookite TiO_2 crystals, J. Mater. Chem. A **3**, 2331 (2015).